Draft version September 25, 2019
Typeset using LaTeX **twocolumn** style in AASTeX63

Nonstationarity of AGN variability: The only way to go is down!

Neven Caplar [1], Theodore Penna,[2] Sean Johnson [1], and Jenny E. Greene[1]

[1] *Department of Astrophysical Sciences, Princeton University, 4 Ivy Ln., Princeton, NJ 08544, USA*
[2] *Department of Physics and Astronomy, Tufts University, Medford, MA 02155, USA*

(Received -; Revised -; Accepted -)

Submitted to ApJL

ABSTRACT

To gain insights into long-term Active Galactic Nuclei (AGN) variability, we analyze an AGN sample from the Sloan Digital Sky Survey (SDSS) and compare their photometry with observations from Hyper Suprime-Cam survey (HSC) observed, $< 14.85 >$ years after SDSS. On average, the AGN are fainter in HSC than SDSS. We demonstrate that the difference is not due to subtle differences in the SDSS versus HSC filters or photometry. The decrease in mean brightness is redshift dependent, consistent with expectations from cosmological time dilation. Moreover, the mean decrease in brightness is stronger for more luminous AGN, and for objects with longer time separation between measurements. The mean decrease in brightness violates the stationarity assumption often invoked in AGN variability studies. We demonstrate that the measured mean brightness decrease and dependence on redshift and Eddington ratio is consistent with simple models of AGN variability on long (Myr, Gyr) timescales. We shot how our results can be used to constrain demographic properties of AGN populations.

Keywords: accretion, accretion disks - black hole physics - methods: data analysis - quasars: general

1. INTRODUCTION

Changing flux levels with time are nearly ubiquitous among Active Galactic Nuclei (AGN). Studies of these luminosity fluctations, i.e., AGN variability, have enabled measurements of central supermassive black hole masses Bentz (2015), added insights on the structure of AGN accretion disks (e.g., (Fausnaugh et al. 2016)) and provide powerful AGN selection techniques Schmidt et al. (2010). AGN variability has been directly observed in large samples on timescale ranging from minutes, to days, years and decades (e.g., MacLeod et al. 2010, 2012; Morganson et al. 2014; Cartier et al. 2015; Caplar et al. 2017; Smith et al. 2018). Through indirect methods and simulations, AGN variability has also been studied on Myr and Gyr scales (e.g., Novak et al. 2011; Bland-Hawthorn et al. 2013; Sartori et al. 2018).

Most of the direct observational studies mentioned above quantify AGN variability as a weakly stationary process i.e., with the assumption that the mean luminosity of statistically large ensembles of AGN does not change with time. Empirically, stochastic variability measured in these studies dominates any possible subtle changes in the mean brightness. From theoretical grounds, the stochastic variability is thought to be reflective of the details of the physics of AGN accretion disks and other nearby structures, while the mean change of luminosity would be connected to long timescale accretion processes thought to have minimal impact on typical survey timescales (Lawrence 2018).

The assumption of stationarity on short timescales differs from the long term studies of AGN activity, which indicate large changes in AGN activity on Myr and Gyr scales. The firmest observational proof comes from the studies of individual "Voorwerp" objects (e.g., Sartori et al. 2016; Johnson et al. 2018) and the He II transverse proximity effect (e.g. Schmidt et al. 2018), which clearly show that some AGN exhibit order-of-magnitude changes in their luminosity on long time-scales.

There has been comparatively little observational research on the deviations from the assumed stationary and symmetric behaviour of AGN variability. Numerous early studies conducted observationally difficult

Corresponding author: Neven Caplar
ncaplar@princeton.edu

searches for potential differences in the variability properties when AGN get brighter versus dimmer (de Vries et al. 2003, 2005; Bauer et al. 2009; Voevodkin 2011), but found little or no evidence for deviations from full symmetry. MacLeod et al. (2012) combined the earliest statistically significant sample of AGN measurements from the Palomar Observatory Sky Surveys (POSS) with the SDSS data. They noted that objects from POSS are dimmer when observed in SDSS. This may be explained by a " Malmquist-like" bias, i.e., the fact that luminosity selected sample of variable objects will necessarily be dimmer in the later survey, even if there is no change in the mean brightness of the underlying sample. A similar conclusion was reached by Rumbaugh et al. (2018) who studied examples of extreme variability by comparing SDSS and Dark Energy Survey measurements. Morganson et al. (2014) also found the decrease of the mean brightness on decade timescales, for the sample of AGN from the SDSS observed in Pan-STARRS1, but attributed this effect to the filter differences.

Here, we use the AGN sample from SDSS and measure their mean brightness in SDSS and HSC. Depth, size, time-separation from SDSS and quality of HSC survey makes is especially suitable for this kind of study. In this work we aim show that AGN exhibit changes in their mean brightness in the redshift and luminosity dependent manner on the timescales accessible with past (SDSS) and current (HSC) surveys.

The code, the data and additional examples are available at github.com/nevencaplar/Nonstationarity.

2. OBSERVATIONS

2.1. *Data*

To study AGN variability on decade timescales, we identified AGN from the SDSS (York et al. 2000) DR7 Quasar catalog (Schneider et al. 2010) that were also observed later by the Hyper Suprime-Cam (HSC; Miyazaki et al. 2018) Subaru Strategic imaging survey. The SDSS survey used a dedicated 2.5-m (Gunn et al. 2006) telescope at Apache Point Observatory to obtain images in 5 optical bands (ugriz) over a large patch ($\sim$10000 deg^2) of Northern sky. For presentation of the photometric calibration and selection function of objects we refer the reader to detailed discussion in Schneider et al. (2010). The HSC survey is a wide-field optical imaging program being conducted with the 8.2 meter Subaru telescope. The second data release (made available in May 2019; Aihara et al. 2019) covers around 300 deg^2 overlapping with the SDSS footprint. The HSC data in 5 optical bands (grizy) is sensitive down to $\approx$ 26th magnitude.

We searched for objects from SDSS AGN catalog in the HSC data and record their g, r and i psf-magnitudes We have excluded all of the objects with any flags showing problems in the calibration. This conservative cut ensures that our conclusions are not driven by possible problems in the brightness measurements in the HSC pipeline. This procedure yields 5919 matched AGN found in both surveys.

2.2. *Main result*

We proceed to measure the difference in the brightness between the two surveys. We split the sample in bins of redshift, where each bin consists of 100 objects. This number enables us to follow the redshift evolution of the trends in some detail, while keeping the uncertainty on the mean brightness change relatively low. For each redshift bin, we then measure the mean and the median difference between the observed psf-magnitude in SDSS and HSC surveys.

The resulting mean change in flux is plotted as a function of redshift in Figure 1. To avoid cluttering the plot we only explicitly show data points at each redshift for measurements in the g-band. The uncertainties on the mean value at each redshift have been derived by bootstraping the underlying 100 AGN in each bin. We choose to present g-band result given that contribution of the host-galaxy light, however small for these bright quasars, will be smallest in the bluest available band. However, results for all 3 bands are very similar. We also show linear fits to the data in all 3 bands, where one can explicitly see the similarity between all of the results. We have also verified that the redshift evolution effect is present if we use median differences instead of mean differences of magnitudes, but the magnitude of the effect is somewhat decreased. For instance, the best fit for the median difference is $-0.139+0.051z$ while for mean difference it is $-0.176+0.06z$. The fact the effect is still present when using the median shows that it cannot fully explained by relatively small number of extremely variable quasars (e.g., MacLeod et al. 2016; Rumbaugh et al. 2018). The difference is consistent with the model in which measured changes of the mean/median flux are the consequence of the long-term AGN behaviour. We also show the linear fit as a function of restframe time separation between two measurements, i.e., as a function of 14.85 years/$(1+z)$, which also provides good explanation for the observed data. We discuss the proposed model further in Section 3.

To ensure that the observed redshift dependence is not a spurious artifact due to differences between two surveys, we conduct four different checks which we list here:

- consideration of filter differences
- constructing a control sample

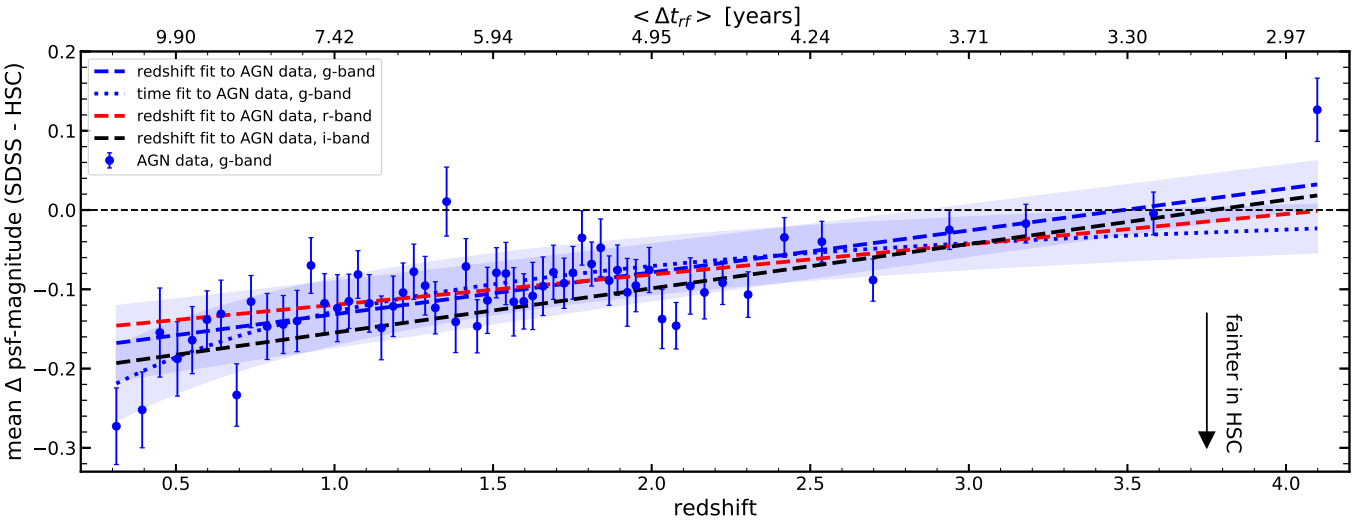

Figure 1. Mean difference in the measured psf-magnitudes for the sample of AGN from SDSS that have been observed in both SDSS and HSC. Blue points shows the data for the g-band, while the blue dashed line and the shaded region show the linear fit as function of redshift to the data and 1-σ uncertainty band. The red and the black dashed lines show the linear fit as a function of redshift in r- and i- bands, respectively. We do not show the data and uncertainty bands for r- and i-band to improve clarity of the figure, but these are comparable to the g-band quantities. The dotted line shows a fit to the g-band data as a function of restframe time-separation between measurements, indicated on the upper axis.

- separating the AGN sample according to brightness
- separating the AGN sample according to the time separation between the SDSS and HSC observations.

We elaborate on each of these procedures in some detail below. For consistency, we always show results for mean difference in g-band and conduct linear fits as a function of redshift, but all of conclusion are applicable to all 3 bands and fitting variables (redshift or restframe time separation).

2.3. *Filter difference and control sample*

We performed two experiments to assess the potential impact of differences in the photometry between the SDSS and HSC surveys which could lead to spurious apparent variability. First, to assess the potential impact of differences in the filter systems on the measured magnitudes, we predicted $g_{\rm SDSS} - g_{\rm HSC}$ for the mean SDSS quasar SED (Vanden Berk et al. 2001) as a function of redshift using the SDSS (Fukugita et al. 1996) and HSC (Kawanomoto et al. 2018) defined system throughput including the filters, telescopes, cameras, and the survey standard atmospheres. Second, we constructed a control sample consisting of non-variable stars with similar colors as the AGN. The stars were taken from the catalog of non-variable objects from the equatorial Stripe 82 presented in Ivezić et al. (2007) which we additionally cleaned by removing suspected AGN from Flesch (2015). For each AGN we find the star (repetition allowed) which minimizes the euclidean distance between the measured magnitudes in the g-, r- and i- bands from SDSS. After that, we treated the catalog of stars that we have created in exactly the same way as we have treated the AGN sample. As, by definition, we expect no change in the brightness of these stars when imaged in the two surveys, any systematic differences between two surveys will be expressed in this comparison. These experiments capture effects both from filter differences and from any differences in the PSF magnitude measurement techniques.

We show the results of this experiment and deduce effects of filter differences in 2. The decrease in mean flux is not present in the control sample of non-variable stars. We emphasize the absence of "redshift" trend in the control sample. This is an expected result, as the different "redshift" for the control sample correspond to only relatively small changes in the mean color of the objects, which does not affect the calibration of the surveys greatly. We also note that the expected filter differences between the two surveys produce relatively small and almost redshift-independent effect. This is due to the small differences between the SDSS (Fukugita et al. 1996) and HSC (Kawanomoto et al. 2018) g-bands,[1] and characteristic power-law SED of a AGN which result in

[1] with $\lambda_{\rm eff}$ = 4770 Å and FWHM = 1379 Å for SDSS versus $\lambda_{\rm eff}$ = 4754 Å and FWHM = 1395 Å for HSC

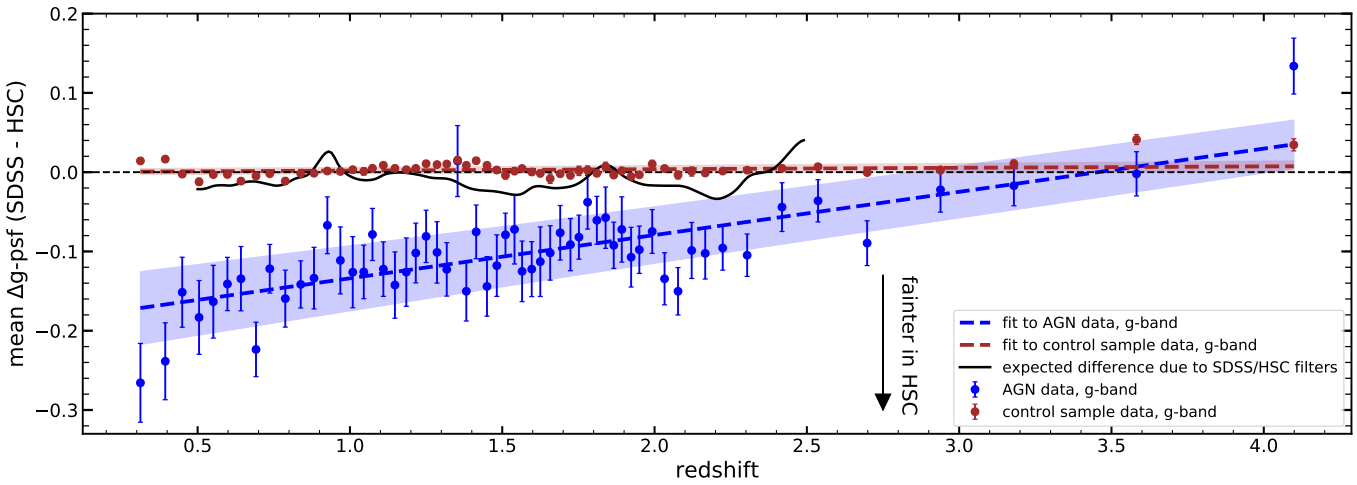

Figure 2. Mean difference in the measured psf-magnitudes for the sample of AGN from SDSS, and the control sample of stars that match these AGN in color. Blue points shows the data for AGN in, while the blue line and the shaded region show the linear fit to the data and 1-σ uncertainty. This is equivalent to the data and fit shown in Figure 1. Maroon points, line and the shaded region show equivalent quantities constructed for the sample of non-variable stars in Stripe 82 region. Black line shows the expected redshift dependence due to filter differences between two surveys.

modest $u-g$ and $g-r$ colors of ≈ -0.2 to 0.3 on the AB system (e.g. Richards et al. 2001). Based on these two tests, we conclude that differences in the survey photometry cannot explain the observed difference between two AGN measurements.

2.4. *Split according to brightness*

We then proceed to study the redshift effect after splitting our sample in brightness. We do this for two separate reasons. Observationally, we would expect that systematic differences between the surveys would be more strongly manifested for objects that have lower brightness, as various errors and uncertainties start to dominate closer to the brightness limit of SDSS survey. Among less luminous AGN, which occur predominantly at lower redshifts, flux from the host galaxy may start to be non-negligible (Shen et al. 2011), which might bias our results. On the other hand, physically, we would expect that the mean brightness change would be larger for brighter AGN, as those AGN are, on average, first imaged in more extreme parts of their life-cycle and we would therefore expect that they will drop more during any given observed time-frame.

We have split the data in each redshift bin in 5 further bins, according to their observed brightness. We then proceed to fit the data in each of these brightness bins with a linear function and show the results of the fitting procedure in Figure 3. As errors on the fit are very similar for all of the 5 bins, we show the mean error on the fit in the separate panel below the main panel. We see that the effect is indeed stronger for the brighter AGN, as we expected from both observational and physical grounds. This makes us even more confident in the physical nature of this effect. We also wish to point out that the observed brightening for the dimmest objects is mostly driven by the few last points at the highest redshifts, and it is not obvious that is also a physical result.

2.5. *Split according to the time separation*

As a final check we separated our sample in the quintiles according to the time-separation between the observations. As both surveys took data over several years, we can look at the data that has been taken, by random chance, at shortest and longest time intervals and compare the results. If the change of mean brightness is mostly due to observational effects we would expect no difference between the short and long separation datasets, while if the difference is physical we would expected to see some difference between these two sets.

This experiment is somewhat complicated by the fact that we, at this stage, are only working with the stacked HSC data, i.e., the measured brightness of any object is a combination of measurements at different times during the duration of the survey. For HSC data we take mean of all of the observation times that go into each stacked observation, and use that "mean time" as the time of the observation. The distribution of time differences between the surveys is roughly normal, with the mean at 14.85 years. We then create a sample out of the data for which the time separation is within shortest time separations quintile (short separation sample) and out of the data which is in the longest time separations quintile (long separation sample). Mean time

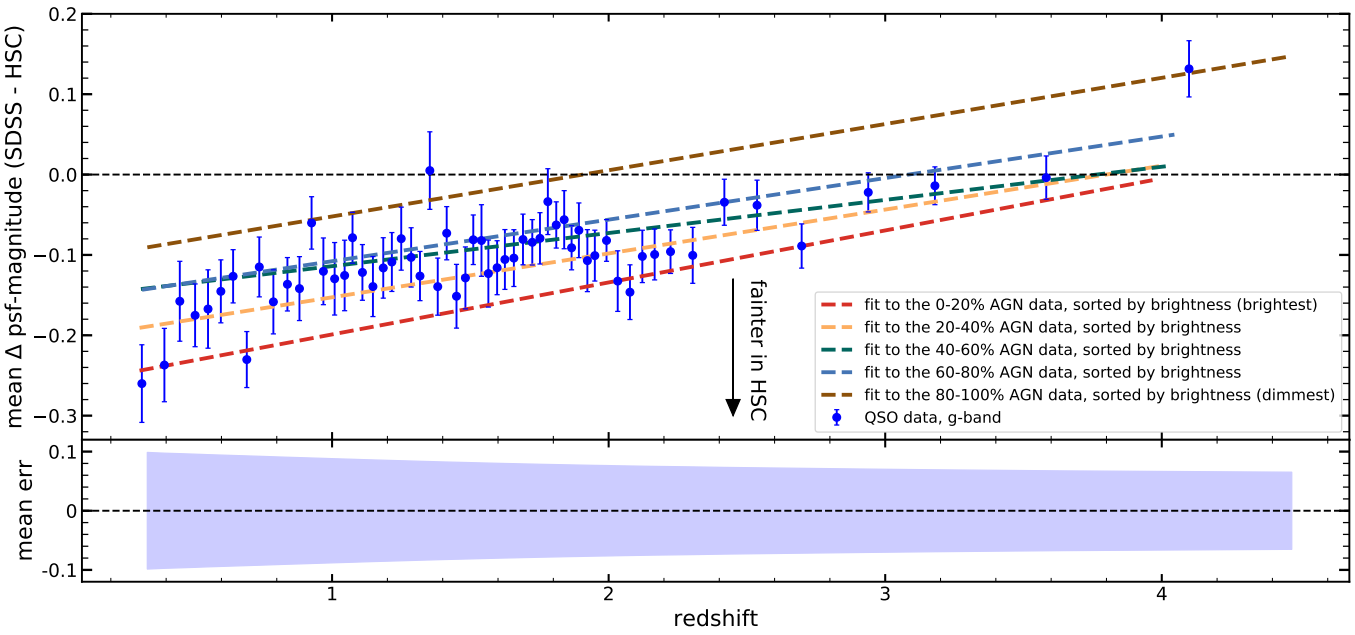

Figure 3. Mean difference in the measured psf-magnitudes in g-band for the sample of AGN separated according to their brightness at each redshift. The blue data shows the data for the whole sample and is the same as in Figure 1. Different colored lines show the results of the linear fit to the subsets of the data, that have been constructed by separating the data at each redshift in quantiles, according to their brightness. Lower panel shows 1-σ uncertainty bands around these linear fits. Note that scaling on y-axis is different than in the upper panel.

separation for the short separation sample is 12.94 years, and for the long separation sample is 16.89 years.

We then proceed as before and study the redshift dependence of each of these samples. We have binned the data in coarser redshift bins in order to preserve statistical power of individual datapoints, given that each of the subsamples contains a fraction of the full data. We show the data, the results of the linear fit to the full data and long/short separations at Figure 4. We see that, in general, long separation data does indeed tend to show larger changes between two surveys. Of course, the results are noisy, which is not unsurprising given the underlying stochastic variability. We also emphasize that given the relatively small differences in the time separation between long and short separation samples the expected differences are also small. In Figure 4 we also show the expected linear fit for the short separation sample, which was derived from the long separation sample by multiplying the slope with the ratio of mean time separations of each sample i.e., with the factor 12.94/16.89. This is a simplified assumption, as mean change of brightness are not necessarily linear with time, but we see that the modifications explains well the magnitude of the observed difference.

3. MODELLING AND DISCUSSION

In this section we wish to indicate to the reader how this effect can be used to constraint parameters of AGN accretion, given the reasonable set of assumptions. Recently Sartori et al. (2019) developed the code which is capable of simulating Eddington ratio-curves with the duration of Myr to Gyr, and the time resolution of 10-100 days. The inputs to the code are probability density function (PDF; in this case this is the Eddington ratio function) and the power spectrum density (PSD). We model the PSD as a broken power, i.e., with

$$PSD(f) = A \times \left[\left(\frac{f}{f_{\rm br}} \right)^{\alpha_{\rm low}} + \left(\frac{f}{f_{\rm br}} \right)^{\alpha_{\rm high}} \right]^{-1} \quad (1)$$

where $f_{\rm br}$ is the break frequency, and $\alpha_{\rm low}$ and $\alpha_{\rm high}$ are the slopes at lower and higher frequencies, respectively (longer and shorter timescales, respectively). While there is agreement in the community that $\alpha_{\rm high} \approx 2$ (except perhaps at shortest scales, <10 days, e.g., Edelson et al. (2014)), the deduced values for $\alpha_{\rm low}$ and $f_{\rm br}$ vary greatly depending on the survey and method used (e.g., MacLeod et al. 2010, 2012; Graham et al. 2014; Kozłowski 2017). Physically, the determination of $f_{\rm br}$ is of great interest as it would be able to provide us with a clue about the physical scale on which the properties of AGN accretion change.

In left panel of Figure 5 we show the expected mean change of the measured brightness during 14.85 years, the average time difference between two measurements, as a function of $f_{\rm br}$ and $\alpha_{\rm low}$. This plot has been done for the systems that are selected at Eddington ratio which is

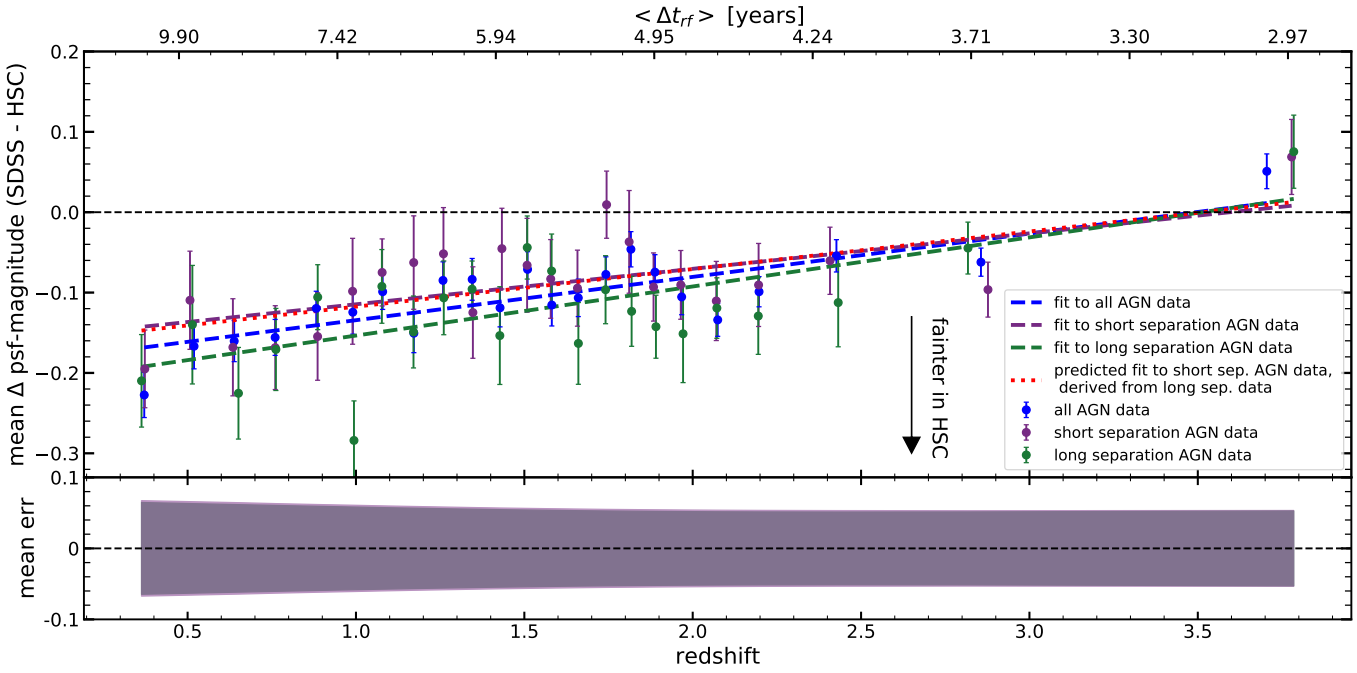

Figure 4. Mean difference in the measured psf-magnitudes in g-band for the sample of AGN split according to the time separation between the measurements. The blue points show the data for the whole sample of AGN in the g-band, while the blue line shows the linear fit to the data. This is equivalent to the data and fit shown in Figure 1, although the binning is different to match binning for short and long separation samples (shown in magenta and green, respectively). The red dotted line shows the simplest "derivation" of the short separation fit, which has been derived from the long separation fit by reducing it by the ratio of the mean time-separations for these two samples (12.94, 16.89 years). The lower panel shows 1-σ uncertainty bands on these linear fits for the short and long separation data. Note that scaling on y-axis is different than in the upper panel.

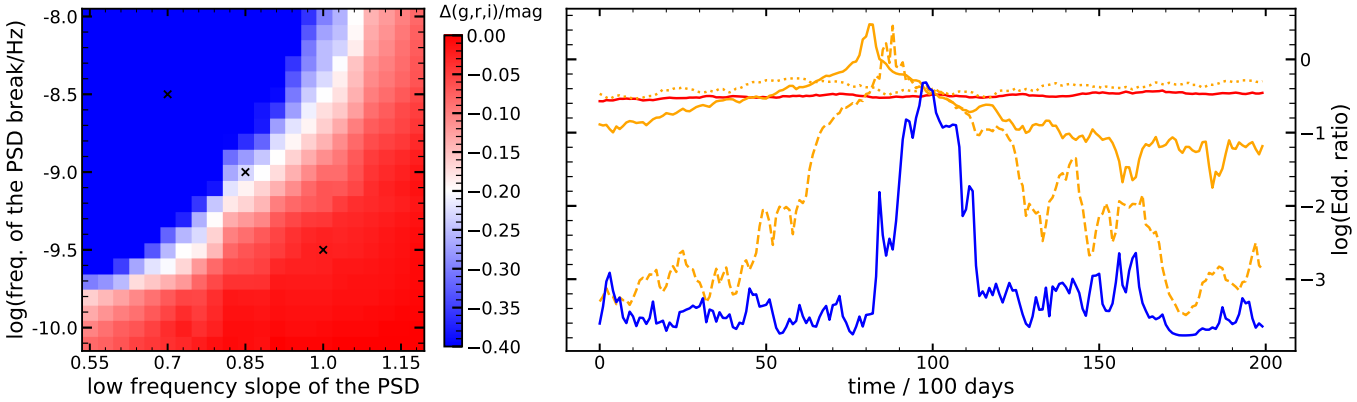

Figure 5. *Left:* The mean change in measured brightness for AGN sampled at 0.5 mag above the brightness cut of a hypothetical survey, and measured again 14.85 years later, as a function of $\alpha_{\rm low}$ and $f_{\rm br}$. *Right:* Typical "light curves" (Eddington ratio) curves, from each of the areas denoted with a small cross on the left hand side. Colors correspond to the colors on the left hand side, where we use orange (instead of white) to color the curves from the middle, observationally plausible, region. We show three curves from the middle region to demonstrate the diversity of behaviours.

0.2 dex (0.5 mag) above the break of the Eddington ratio distributions, which mimics the SDSS observational cut. We can see the observation of mean brightness change defines very specific range of allowed values in this parameter space. The two parameters are somewhat degenerate - observationally there is little difference is the process decorrelates quickly at longer timescale (small $\alpha_{\rm low}$ and large $f_{\rm br}$) or slowly at shorter timescales (large $\alpha_{\rm low}$ and small $f_{\rm br}$ - see also Figure 12. in Caplar & Tacchella 2019). On the right hand side of 5 we show representative "light curves" (Eddington ratio curves) from different regions of the parameters space. In particular, we emphasize the wide variety of the behaviours for the curves which are consistent with the observed changes in the mean brightness, which is reminiscent of the wide diversity of observed variability behaviours for AGN.

Qualitatively, as indicated before, this model also explains why the most luminous objects at lowest redshift are more likely to get dimmer - as they are already occupy the uppermost edges of the probability density function they have the most time and are far more likely to get dimmer and move to more probable regions of the parameter space. In other words, for the brightest AGN the only way to go is down!

In future we aim to improve observational constraints and finely map time dependence by incorporating information from different surveys, such as POSS, Pan-STARRS and Zwicky Transient Factory. We also aim to use this full information and luminosity dependence of the effects to place fine constraint on several physical parameters of AGN accretion, in the manner similar as shortly described above.

ACKNOWLEDGEMENTS

During preparation of this manuscript, we have benefited from useful discussions with Laurent Eyer, Željko Ivezić, Chelsea MacLeod, Sophie Reed, Lia Sartori, John Silvermann and Krzysztof Suberlak. We especially thank Yusra AlSayyad who prepared the filter flags used when retrieving the HSC data.

This research made use of NASA's Astrophysics Data System (ADS), the arXiv.org preprint server, the Python plotting library `matplotlib` (Hunter 2007) and `astropy`, a community-developed core Python package for Astronomy (Astropy Collaboration et al. 2013).

REFERENCES

Aihara, H., AlSayyad, Y., Ando, M., et al. 2019, arXiv e-prints, arXiv:1905.12221. https://arxiv.org/abs/1905.12221

Astropy Collaboration, Robitaille, T. P., Tollerud, E. J., et al. 2013, A&A, 558, A33, doi: 10.1051/0004-6361/201322068

Bauer, A., Baltay, C., Coppi, P., et al. 2009, ApJ, 696, 1241, doi: 10.1088/0004-637X/696/2/1241

Bentz, M. C. 2015, arXiv e-prints, arXiv:1505.04805. https://arxiv.org/abs/1505.04805

Bland-Hawthorn, J., Maloney, P. R., Sutherland , R. S., & Madsen, G. J. 2013, ApJ, 778, 58, doi: 10.1088/0004-637X/778/1/58

Caplar, N., Lilly, S. J., & Trakhtenbrot, B. 2017, ApJ, 834, 111, doi: 10.3847/1538-4357/834/2/111

Caplar, N., & Tacchella, S. 2019, MNRAS, 487, 3845, doi: 10.1093/mnras/stz1449

Cartier, R., Lira, P., Coppi, P., et al. 2015, ApJ, 810, 164, doi: 10.1088/0004-637X/810/2/164

de Vries, W. H., Becker, R. H., & White, R. L. 2003, AJ, 126, 1217, doi: 10.1086/377486

de Vries, W. H., Becker, R. H., White, R. L., & Loomis, C. 2005, AJ, 129, 615, doi: 10.1086/427393

Edelson, R., Vaughan, S., Malkan, M., et al. 2014, ApJ, 795, 2, doi: 10.1088/0004-637X/795/1/2

Fausnaugh, M. M., Denney, K. D., Barth, A. J., et al. 2016, ApJ, 821, 56, doi: 10.3847/0004-637X/821/1/56

Flesch, E. W. 2015, PASA, 32, e010, doi: 10.1017/pasa.2015.10

Fukugita, M., Ichikawa, T., Gunn, J. E., et al. 1996, AJ, 111, 1748, doi: 10.1086/117915

Graham, M. J., Djorgovski, S. G., Drake, A. J., et al. 2014, MNRAS, 439, 703, doi: 10.1093/mnras/stt2499

Gunn, J. E., Siegmund, W. A., Mannery, E. J., et al. 2006, AJ, 131, 2332, doi: 10.1086/500975

Hunter, J. D. 2007, Computing in Science and Engineering, 9, 90, doi: 10.1109/MCSE.2007.55

Ivezić, Ž., Smith, J. A., Miknaitis, G., et al. 2007, AJ, 134, 973, doi: 10.1086/519976

Johnson, S. D., Chen, H.-W., Straka, L. A., et al. 2018, ApJL, 869, L1, doi: 10.3847/2041-8213/aaf1cf

Kawanomoto, S., Uraguchi, F., Komiyama, Y., et al. 2018, PASJ, 70, 66, doi: 10.1093/pasj/psy056

Kozłowski, S. 2017, A&A, 597, A128, doi: 10.1051/0004-6361/201629890

Lawrence, A. 2018, Nature Astronomy, 2, 102, doi: 10.1038/s41550-017-0372-1

MacLeod, C. L., Ivezić, Ž., Kochanek, C. S., et al. 2010, ApJ, 721, 1014, doi: 10.1088/0004-637X/721/2/1014

MacLeod, C. L., Ivezić, Ž., Sesar, B., et al. 2012, ApJ, 753, 106, doi: 10.1088/0004-637X/753/2/106

MacLeod, C. L., Ross, N. P., Lawrence, A., et al. 2016, MNRAS, 457, 389, doi: 10.1093/mnras/stv2997

Miyazaki, S., Komiyama, Y., Kawanomoto, S., et al. 2018, PASJ, 70, S1, doi: 10.1093/pasj/psx063

Morganson, E., Burgett, W. S., Chambers, K. C., et al. 2014, ApJ, 784, 92, doi: 10.1088/0004-637X/784/2/92

Novak, G. S., Ostriker, J. P., & Ciotti, L. 2011, ApJ, 737, 26, doi: 10.1088/0004-637X/737/1/26

Richards, G. T., Fan, X., Schneider, D. P., et al. 2001, AJ, 121, 2308, doi: 10.1086/320392

Rumbaugh, N., Shen, Y., Morganson, E., et al. 2018, ApJ, 854, 160, doi: 10.3847/1538-4357/aaa9b6

Sartori, L. F., Schawinski, K., Trakhtenbrot, B., et al. 2018, MNRAS, 476, L34, doi: 10.1093/mnrasl/sly025

Sartori, L. F., Trakhtenbrot, B., Schawinski, K., et al. 2019, arXiv e-prints, arXiv:1909.06374. https://arxiv.org/abs/1909.06374

Sartori, L. F., Schawinski, K., Koss, M., et al. 2016, MNRAS, 457, 3629, doi: 10.1093/mnras/stw230

Schmidt, K. B., Marshall, P. J., Rix, H.-W., et al. 2010, ApJ, 714, 1194, doi: 10.1088/0004-637X/714/2/1194

Schmidt, T. M., Hennawi, J. F., Worseck, G., et al. 2018, ApJ, 861, 122, doi: 10.3847/1538-4357/aac8e4

Schneider, D. P., Richards, G. T., Hall, P. B., et al. 2010, AJ, 139, 2360, doi: 10.1088/0004-6256/139/6/2360

Shen, Y., Richards, G. T., Strauss, M. A., et al. 2011, ApJS, 194, 45, doi: 10.1088/0067-0049/194/2/45

Smith, K. L., Mushotzky, R. F., Boyd, P. T., et al. 2018, ApJ, 857, 141, doi: 10.3847/1538-4357/aab88d

Vanden Berk, D. E., Richards, G. T., Bauer, A., et al. 2001, AJ, 122, 549, doi: 10.1086/321167

Voevodkin, A. 2011, arXiv e-prints, arXiv:1107.4244. https://arxiv.org/abs/1107.4244

York, D. G., Adelman, J., Anderson, John E., J., et al. 2000, AJ, 120, 1579, doi: 10.1086/301513